

Accelerated dephosphorylation of adenosine phosphates and related compounds in the presence of nanocrystalline cerium oxide

Pavel Janoš^{*a}, Iveta Lovászová^a, Jan Pfeifer^a, Jakub Ederer^a, Marek Došek^a, Tomáš Loučka^a, Jiří Henych^{a,b}, Zdeňka Kolská^c, David Milde^d, Tomáš Opletal^d

^a Faculty of the Environment, University of Jan Evangelista Purkyně, Králova Výchina 7, 400 96 Ústí nad Labem, Czech Republic

^b Institute of Inorganic Chemistry AS CR v.v.i., 25068 Řež, Czech Republic

^c Materials Centre of Usti, Faculty of Science, University of Jan Evangelista Purkyně, České Mládeže 8, 400 96 Ústí nad Labem, Czech Republic

^d Regional Centre of Advanced Technologies and Materials, Department of Analytical chemistry, Faculty of Science, Palacký University, 17. listopadu 12, CZ 771 46 Olomouc, Czech Republic

Supporting Information

Content

1. Measurements of dephosphorylating activity – experimental details	2
HPLC analyses	2
Dephosphorylating measurements	4
Quality control and uncertainty estimation	5
2. SEM images	7
3. TEM images	9
4. High resolution XPS spectra	10
5. Kinetics of the dephosphorylation	12
6. Interactions of cerium oxide with NAD	16

1. Measurements of dephosphorylating activity – experimental details

HPLC analyses

Concentrations of ATP and related compounds, as well as their products of dephosphorylation and reaction intermediates, were determined by liquid chromatography using the LaChrom HPLC system (Merck/Hitachi) consisting of the L-7100 pump, the L-7400 variable wavelength UV/Vis detector operating at 240 nm, the Rheodyne 7725i injection valve with 20 μ L sampling loop and the SeQuant ZIC-HILIC column (Merck, Darmstadt, Germany) 150 x 4.6 mm, packed with zwitterionic stationary phase bound to silica, 3.5 μ m. Basic operational and performance characteristics are given in Table S1, example of the separation is given in Fig. S1.

Table S1. Mobile phase composition and performance characteristics of the HPLC method

Substrate	Mobile phase	Analyte	t _R (min)	LOD (mg/L)	RSD (%)
ATP	acetonitrile/acetate buffer 0.05 mol/L, pH 5.01 65/35 (v/v)	adenosine	2.20	5.57	6.5
		AMP	4.93	4.80	6.6
		ADP	6.37	3.05	10.9
		ATP	7.40	3.26	12.5
IMP	acetonitrile/acetate buffer 0.05 mol/L, pH 5.01 65/35 (v/v)	inosine	1.83	4.24	7.13
		IMP	9.75	7.64	11.6
CMP	acetonitrile/acetate buffer 0.05 mol/L, pH 5.01 60/40 (v/v)	cytidine	2.85	3.82	6.8
		CMP	6.30	4.03	6.9
GMP	acetonitrile/acetate buffer 0.05 mol/L, pH 5.01 45/55 (v/v)	guanosine	ND	ND	ND
		GMP	3.42	5.56	9.4
TPP	acetonitrile/acetate buffer 0.05 mol/L, pH 5.01 45/55 (v/v)	thiamine	3.62	6.04	8.4
		TMP	5.24	5.12	12.2
		TPP	4.37	5.25	11.3

ATP – adenosine triphosphate; ADP- adenosine diphosphate, AMP – adenosine monophosphate; IMP – inosine 5'- monophosphate; CMP – cytidine 5'-monophosphate; GMP 5'-guanosine monophosphate; TPP – thiamine pyrophosphate; TMP – thiamine monophosphate; ND – not detected (sparingly soluble); t_R – retention time; LOD – limit of detection; RSD – relative standard deviation of repeatability (n=7)

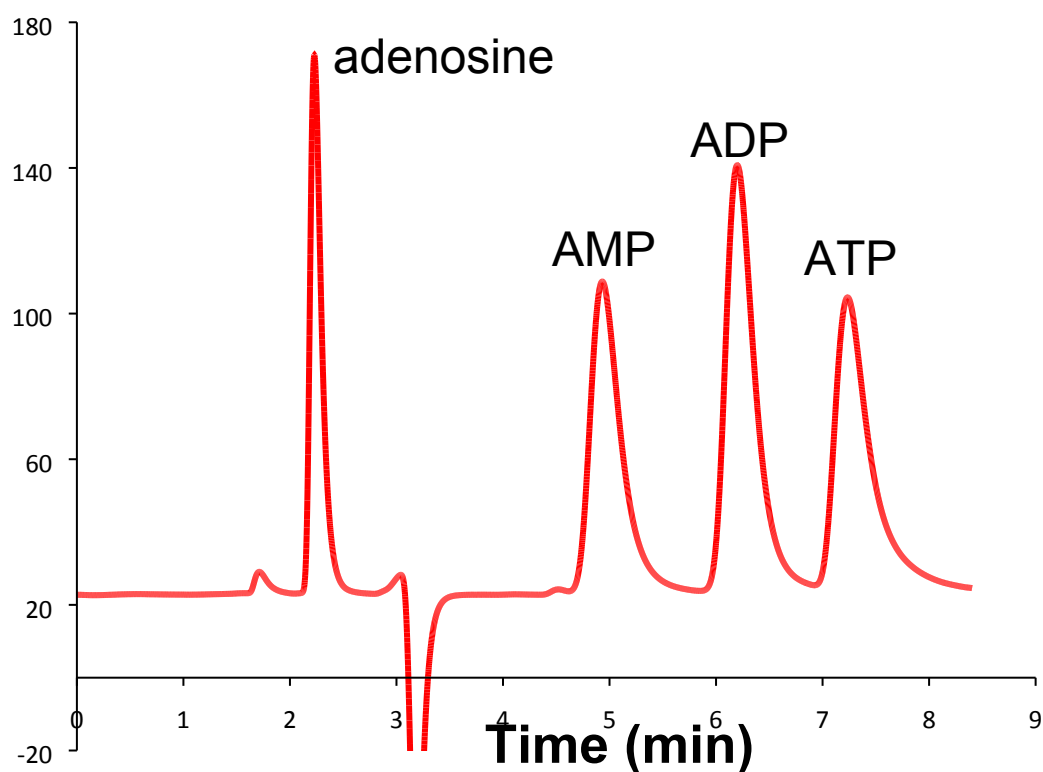


Fig. S1. HPLC separation of model mixture. Concentrations: 0.1 mmol/L of adenosine, 0.2 mmol/L of AMP, ADP and ATP.

Alternatively, the Triart Diol-HILIC column (YMC Comp., Kyoto, Japan) 150×3 mm, $5 \mu\text{m}$, was used under similar conditions (mobile phase composition, detection); comparable performance characteristics were achieved with this column.

Some examples of the chromatographic analyses are shown in **Fig. S2**. It is shown in **Fig. S2a** that ATP is dephosphorylated partially in the presence of the in-house cerium oxide (denoted as $\text{CeO}_2\text{-}500^\circ\text{C}$ here). The peaks corresponding to the dephosphorylation products (ADP, AMP and adenosine) are clearly visible on the chromatogram. Only minor amounts of the dephosphorylation products were detected when the experiment was performed in the presence of the commercial nanoceria MKN-025, whereas the blank experiments confirmed that the dephosphorylation does not proceed in the absence of cerium oxide.

In **Fig S2b**, the dephosphorylating activity of the cerium oxide was compared with the activities of oxides of other REEs (lanthanum, praseodymium and neodymium) that were prepared in a similar way as the in-house cerium oxide used in this study. As can be seen, AMP was dephosphorylated and an (almost) equivalent amount of adenosine liberated in the presence cerium oxide, whereas the oxides of other REEs exhibited negligible dephosphorylating activity under identical conditions (note that the peak of AMP remained almost unchanged in the presence of lanthanum oxide, praseodymium oxide and neodymium oxide, whereas it disappeared completely in the presence of cerium oxide, and a new peak was identified as adenosine).

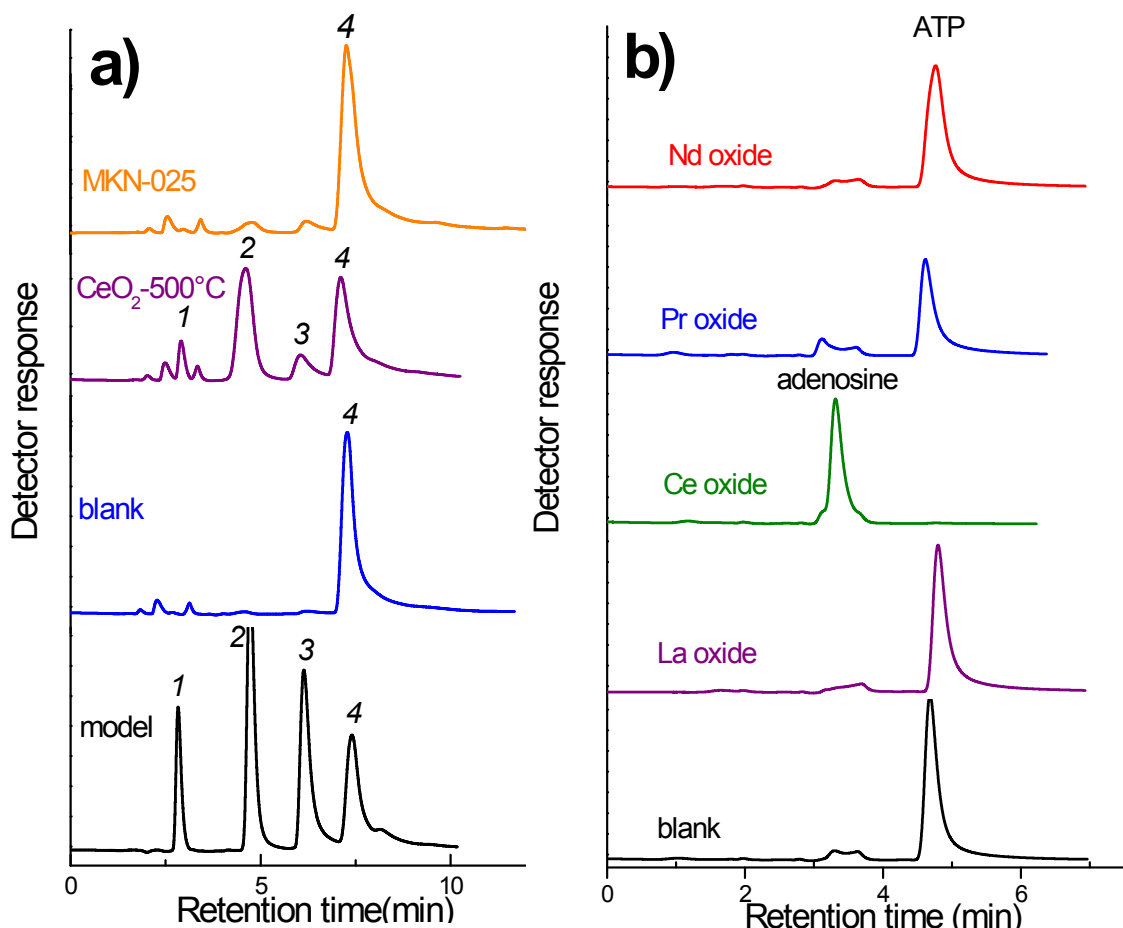


Fig. S2. a) Dephosphorylation of ATP in the presence of cerium oxide annealed at 500°C and commercial nanoceria MKN-025. Initial concentrations of AMP 0.002 mol/L; 0.04 mol/l TRIS buffer with pH = 7.22. Concentrations of cerium oxides 0.5 g/100 mL; equilibrating time 48 hours. Chromatographic conditions: Column YMC-TRIART DIOL-HILIC, 150 × 4.6 mm, 5 μm; mobile phase acetonitrile/ammonium acetate 0.10 mol/L, pH 5.00 (67/33, v/v); detection UV 240 nm. Peak identification: 1 – adenosine; 2 – AMP; 3 – ADP; 4 – ATP. b) Dephosphorylation of ATP in the presence of cerium oxide annealed at 500°C and oxides of some other REEs prepared in a similar way. Initial concentrations of AMP 0.002 mol/L; 0.04 mol/l TRIS buffer with pH = 7.22. Concentrations of REEs oxides 2.0 g/100 mL; equilibrating time 48 hours. Chromatographic conditions: Column YMC-TRIART DIOL-HILIC, 150 × 4.6 mm, 5 μm; mobile phase acetonitrile/ammonium acetate 0.01 mol/L, pH 5.01 (75/25, v/v); detection UV 240 nm.

Dephosphorylating measurements

The long-term dephosphorylation experiments were carried out in 20 mL glass vials containing 10 mL of a 0.002 mol/L ATP solution in TRIS buffer (concentration of 0.04 mol/L, pH 7.22). The kinetic experiments were initiated by the addition of a known amount of cerium oxide (typically 0.05 g). The closed glass vials were wrapped in aluminium foil to protect the reaction mixture from sunlight and then agitated on a horizontal shaker with an agitation intensity of 2 rps. At pre-determined time intervals, small amounts (0.1-0.5 mL) of the reaction mixture were removed, acidified with 1 mL of formic acid (1%) and diluted to 5 mL with acetonitrile. Cerium oxide was separated by centrifugation (4000 rpm, 5 min), and the supernatant was analyzed immediately by liquid chromatography. Simultaneously, blank experiments were carried out in the same arrangement without cerium oxide. The short-term experiments were carried out in a beaker covered with aluminium foil. Appropriate amounts

of the TRIS buffer and ATP stock solution were mixed together to produce a mixture with an initial ATP concentration of 0.002 mol/L, buffer concentration of 0.04 mol/L and pH of 7.22. The mixture was agitated with a magnetic stirrer. The kinetic experiments were initiated by the addition of a known amount of cerium oxide (ranging from 0.5 to 2 g per 100 mL). The liquid chromatographic analyses were performed in a similar way as described above. The mode of agitation was confirmed to not significantly affect the dephosphorylation rate. All the experiments were carried out in an air-conditioned box at $22\pm 1^\circ\text{C}$. Alternatively, TRIS buffers with the same concentration (0.04 mol/L) but different pH values (6.00, 8.00 or 9.00) or acetate buffers with the same concentration but a pH of 4.00 or 5.00 were used.

Quality control and uncertainty estimation

As a part of the validation study preceding the dephosphorylating experiments, the main performance characteristics of the chromatographic method were determined including standard deviations of repeatability. This parameter encompasses all uncertainty contributions related to the chromatographic measurements including the sample pre-treatment (pH adjustment, dilution, centrifugation); the respective values are summarized in Table S1.

Several kinds of the quality-control (QC) samples were used regularly to check the quality of the chromatographic measurements, such as reagent blanks and in-house reference materials consisting of the analyte solutions daily prepared independently on the calibration standards.

The dephosphorylating experiments were performed in duplicate. A consistency of the experimental data was evaluated by a visual inspection of the dephosphorylating curves. In the case of inconsistency, the whole dephosphorylating experiment was repeated, again in duplicate. The averages from the duplicate measurements were plotted against the reaction time to obtain the dephosphorylating dependencies. An uncertainty arising from the duplicate experiments was combined with the uncertainty of chromatographic measurements according to a general rule $u_{T,rel} = \sqrt{u_{D,rel}^2 + u_{C,rel}^2}$. The experimental data from the dephosphorylating experiments were plotted as an average from duplicate measurements accompanied by an uncertainty (error bar) expressed as a standard deviation.

Simultaneously with every dephosphorylating experiment, the blank experiments were performed in the same experimental arrangement without cerium oxide. As an example, the dephosphorylating experiments at various pH values are shown in the following figure together with the respective blank experiments.

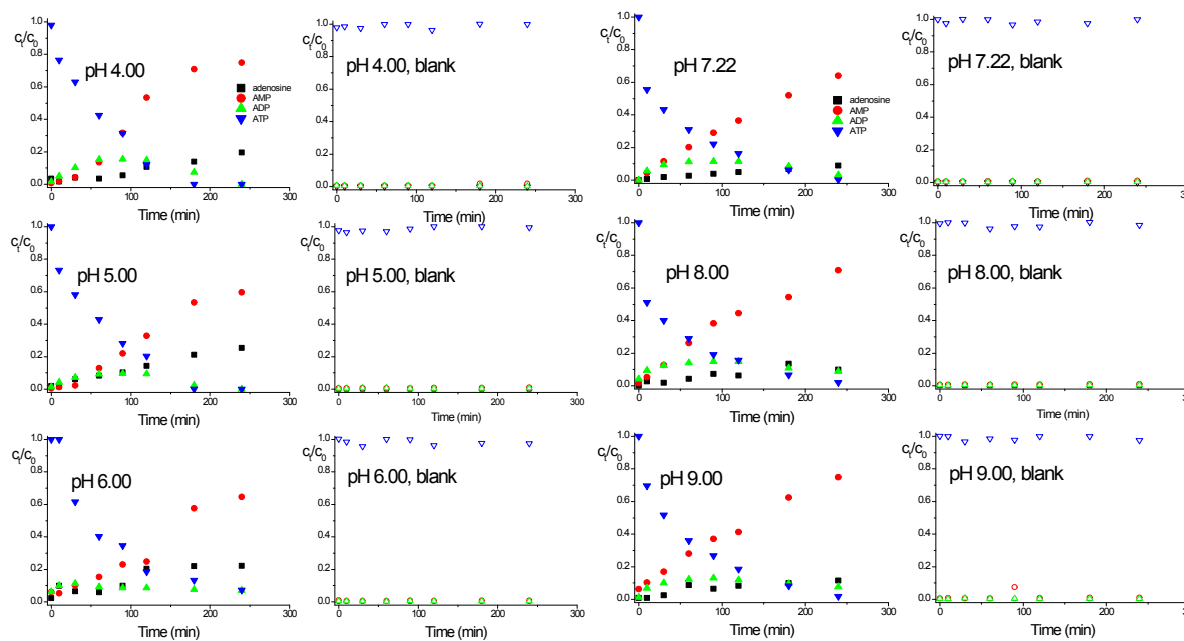
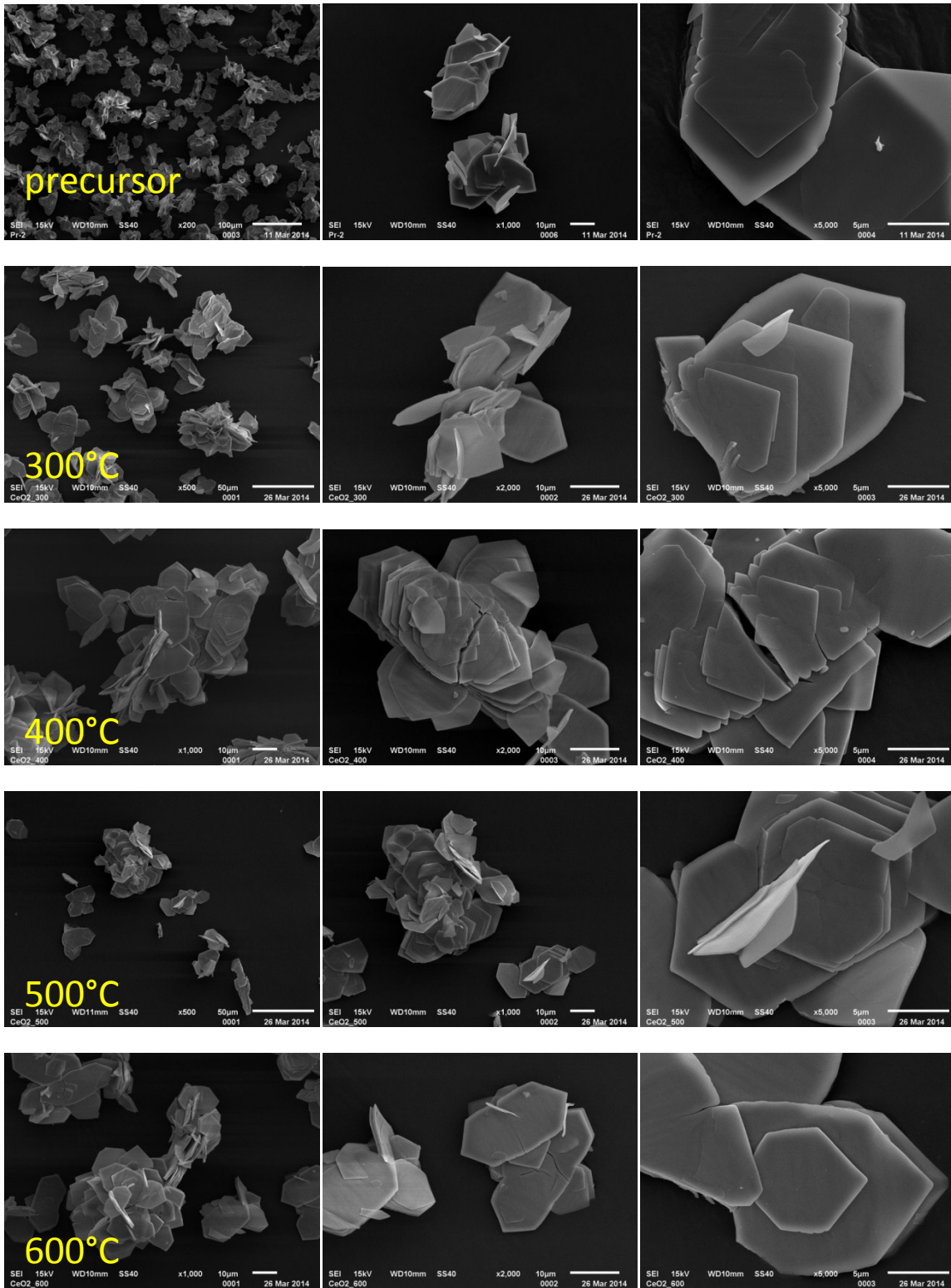


Fig. S3. Dephosphorylation of ATP at various pH values in the presence of cerium oxide annealed at 500°C. Initial concentration of ATP, 0.002 mol/L; concentration of cerium oxide, 0.5 g/100 mL (left columns); TRIS buffer, 0.04 mol/L and pH = 7.22. Right columns (open symbols) – blank experiments. c_i/c_0 = concentrations of individual species divided by the initial concentration of ATP.

2. SEM images



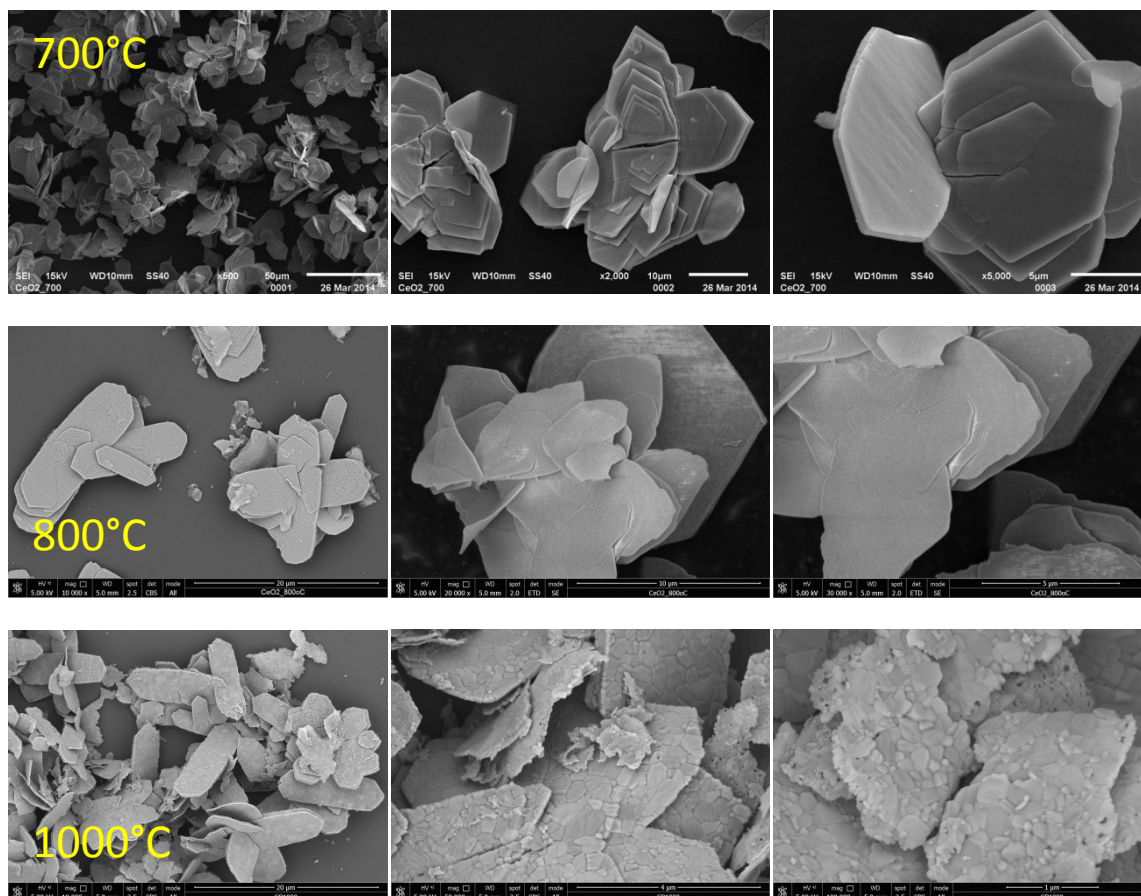


Fig. S4. SEM images of the carbonate precursor (first row) and cerium oxides annealed at various temperatures.

3. TEM images

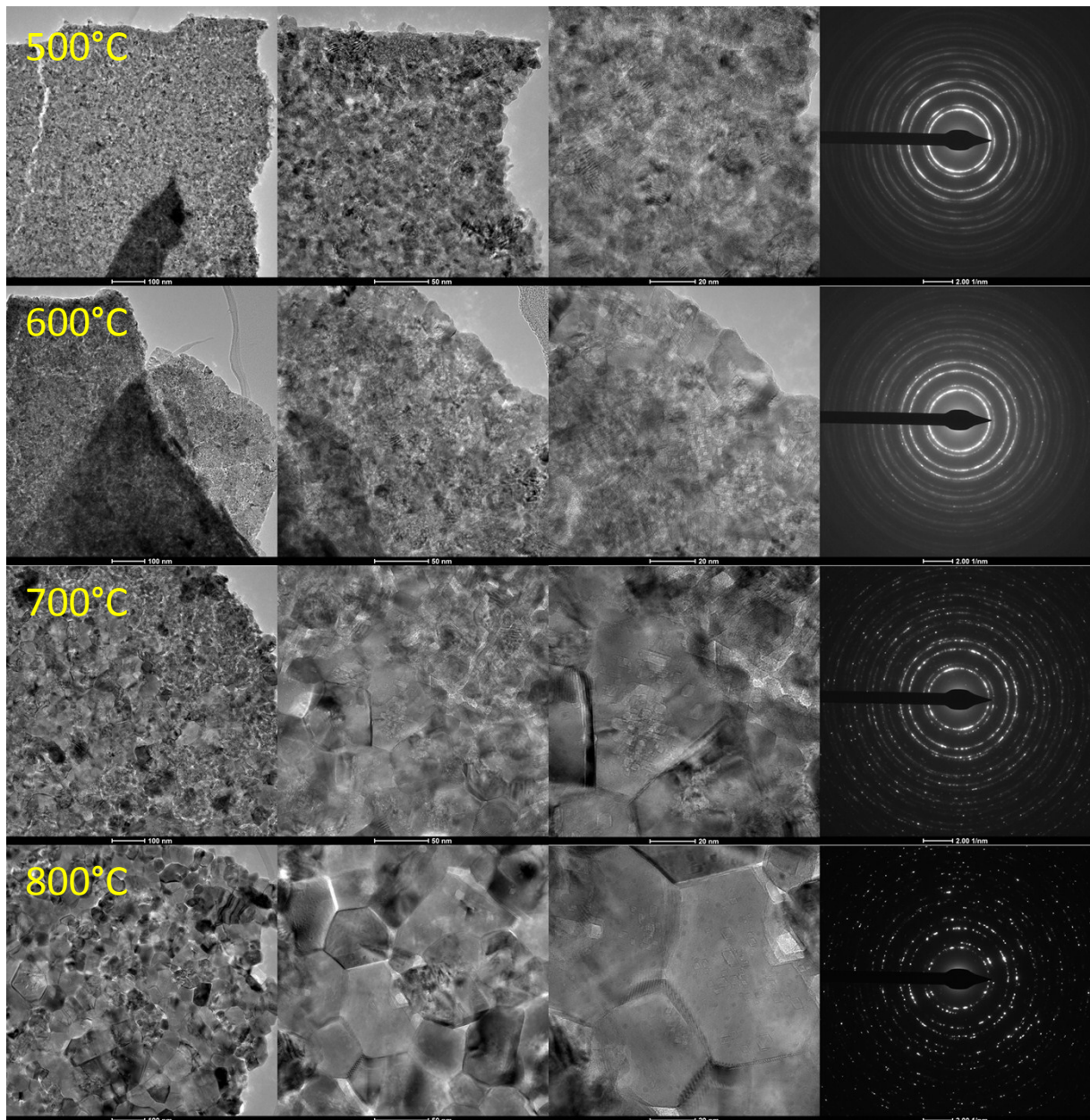


Fig. S5. TEM images of cerium oxides annealed at various temperatures. The TEM images together with the diffraction patterns (right column) suggest that the cerium oxide annealed at lower temperatures consists of a large number of small particles, whereas the cerium oxide annealed at higher temperatures consists of a small number of large particles. (The number of particles may be related the intensity of the diffraction lines.)

4. High resolution XPS spectra

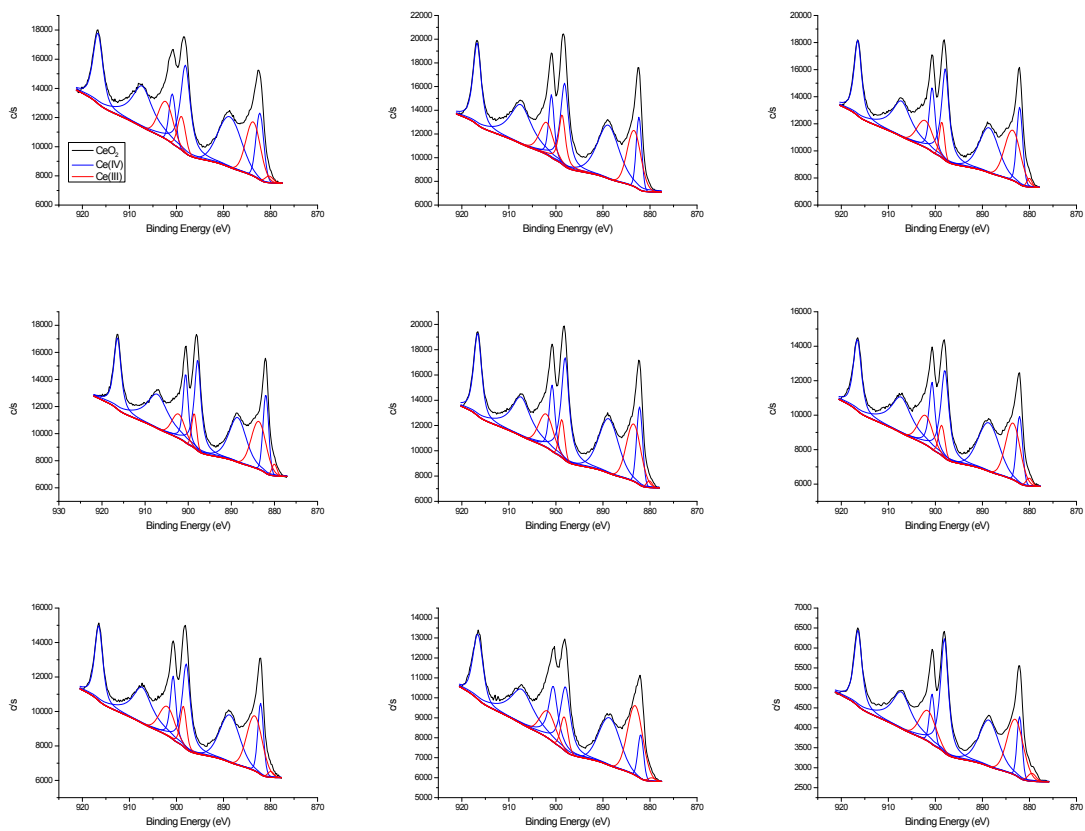


Fig. S6. High resolution XPS spectra Ce 3d for cerium oxide annealed at various temperatures ranging from 200 (top-left) to 1000°C (right – down).

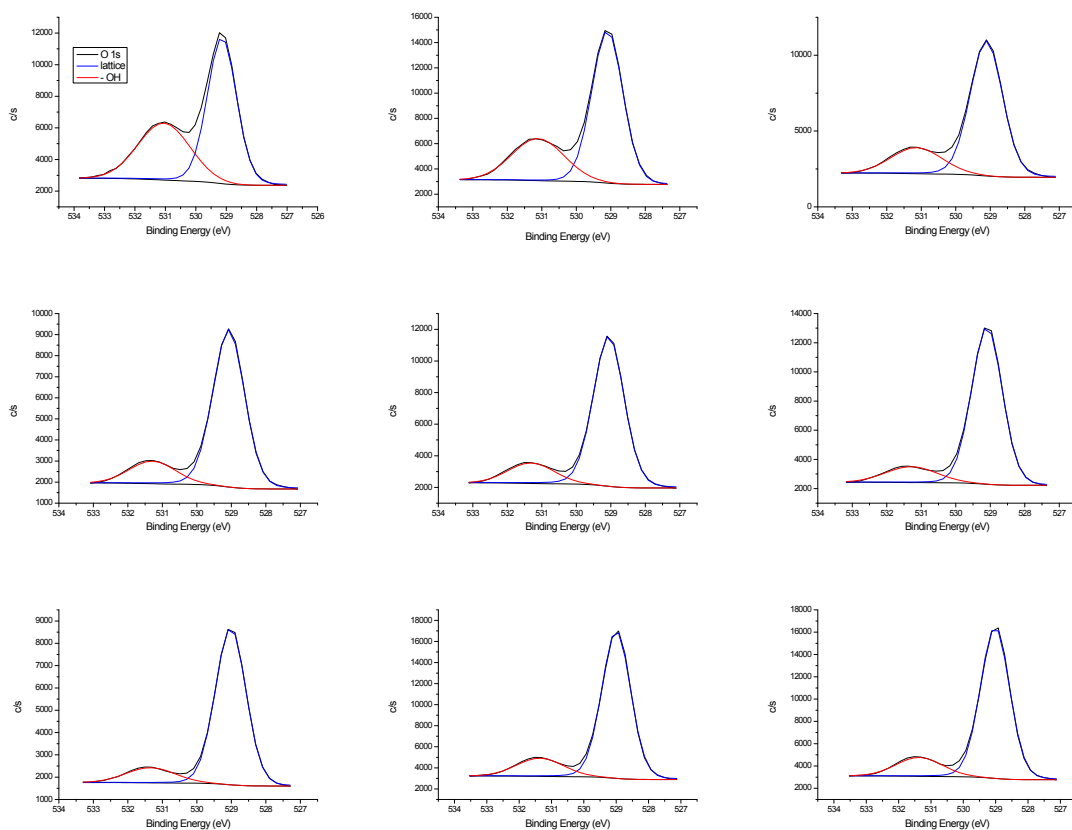


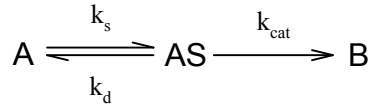
Fig. S7. High resolution XPS spectra O 1s for cerium oxide annealed at various temperatures ranging from 200 (top-left) to 1000°C (right – down).

Table S2. Cerium and oxygen speciation in cerium oxide calculated from XPS spectra

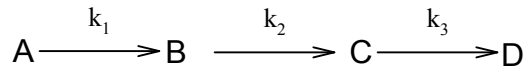
Temperature of calcination (°C)	Ce(IV)	Ce(III)	O-lattice	O-OH
200	76.47	23.53	60.18	39.82
300	75.54	24.46	68.97	31.03
400	76.59	23.41	77.51	22.49
500	78.33	21.67	82.81	17.19
600	77.40	22.60	83.68	16.32
700	77.07	22.93	85.96	14.04
800	74.36	25.64	86.90	13.10
900	73.50	26.50	84.45	15.55
1000	84.21	15.79	84.38	15.62

5. Kinetics of the dephosphorylation

Dephosphorylation of adenosine phosphates can be described by a well-known Michaelis-Menten model for enzymatic catalysis or by an almost identical Langmuir-Hinshelwood model of heterogeneous catalysis:



Even in its basic form, this model gives rather complex rate equations where the reaction order is not clear. However, in the first approximation, the dephosphorylation of ATP to adenosine di- and mono-phosphate, and finally to adenosine may be described as a set of subsequent pseudo first-order reactions



$$-\frac{d c_A}{d t} = k_1 c_A \quad (1)$$

$$\frac{d c_B}{d t} = k_1 c_A - k_2 c_B \quad (2)$$

$$\frac{d c_C}{d t} = k_2 c_B - k_3 c_C \quad (3)$$

$$\frac{d c_D}{d t} = k_3 c_C \quad (4)$$

from which time dependencies for all compounds can be explicitly expressed:

$$c_A = c_A^0 \exp(-k_1 t) \quad (5)$$

$$c_B = c_A^0 \frac{k_1}{k_2 - k_1} [\exp(-k_1 t) - \exp(-k_2 t)] \quad (6)$$

$$c_C = c_A^0 [a \exp(-k_1 t) - b \exp(-k_2 t) + c \exp(-k_3 t)] \quad (7)$$

$$c_D = k_3 c_A^0 \left[\frac{a}{k_1} (1 - \exp(-k_1 t)) - \frac{b}{k_2} (1 - \exp(-k_2 t)) + \frac{c}{k_3} (1 - \exp(-k_3 t)) \right] \quad (8)$$

where

$$a = \frac{k_1 k_2}{(k_2 - k_1)(k_3 - k_1)} \quad (9)$$

$$b = \frac{k_1 k_2}{(k_2 - k_1)(k_3 - k_2)} \quad (10)$$

$$c = \frac{k_1 k_2}{(k_3 - k_1)(k_3 - k_2)} \quad (11)$$

The respective time dependencies are shown schematically in the following figure:

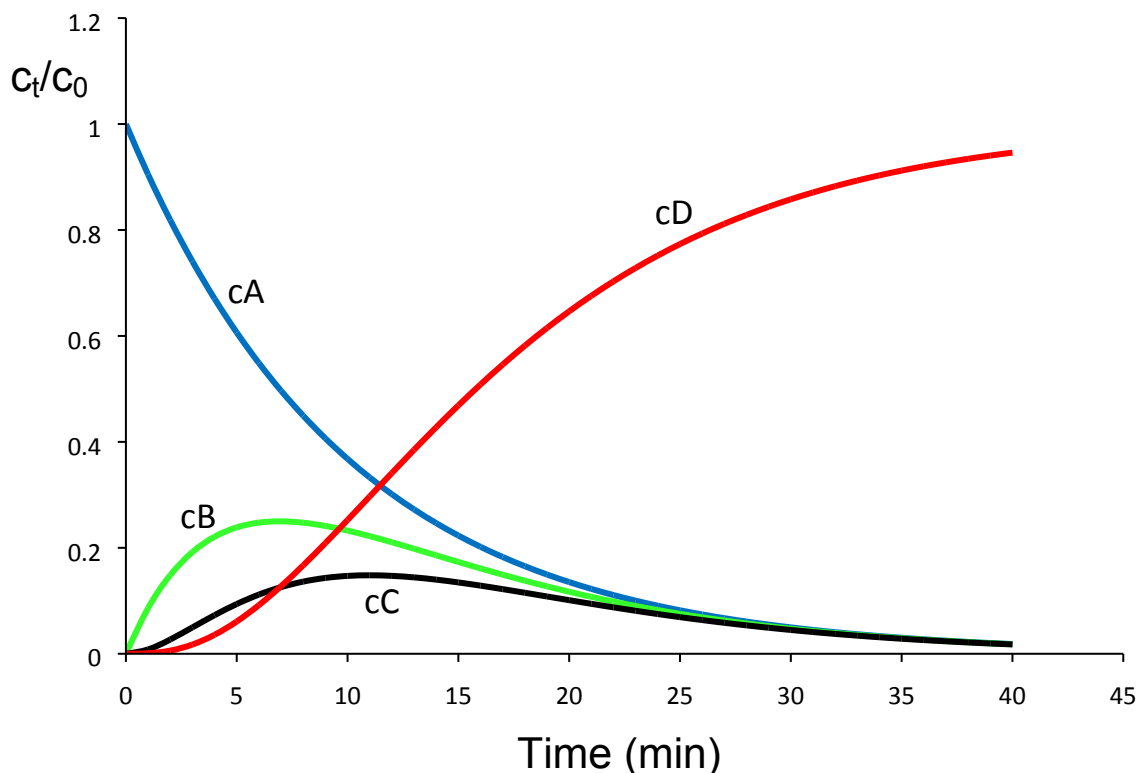


Fig. S8. Kinetics of the ATP dephosphorylation – model calculation for $c_A^0 = 1$; $k_1 = 0.1$; $k_2 = 0.2$, $k_3 = 0.3$

Experimental dependencies comply well (at least qualitatively) with the proposed model, as shown in Fig. S9. The first-order kinetic equation was used successfully to estimate the rate constants for the ATP disappearance in the presence of various cerium oxides (see Fig. 4 in the main text); the respective model parameters are listed in Table S3.

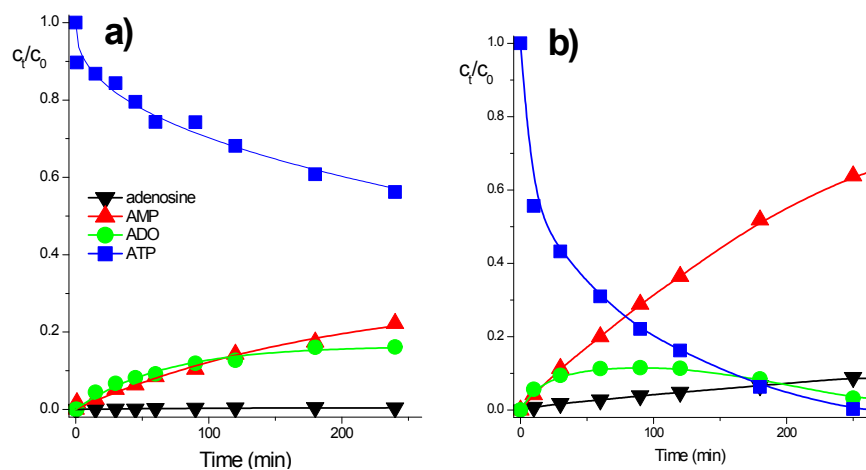


Fig. S9. Kinetics of the ATP dephosphorylation in the presence of cerium oxide annealed at 500°C. Initial concentrations of ATP 0.002 mol/L,; 0.04 mol/l TRIS buffer with pH = 7.22. Concentrations of cerium oxide 1.0 g/100 mL (a) and 2.0 g/100 mL (b).

Table S3. Parameters of the first-order equation (Eq.(5)) ^{a)}

	A	B	C	D	E1	E2	E3	E4	E5	E6
1	Model	Louka01 (User)								
2	Equation	A*exp(-k1*x)								
3	Reduced Chi-Sqr	0.00166	2.00072E-4	0.00162	2.82783E-4	6.65758E-4	8.26799E-4	2.5934E-4	3.55254E-4	1.06965E-4
4	Adj. R-Square	0.9875	0.99849	0.98777	0.99821	0.99598	0.99386	0.99636	0.96922	0.9689
5			Value	Standard Error						
6	200 °C	A	0.97686	0.03806						
7		k1	0.02697	0.00219						
8	300 °C	A	0.99269	0.0131						
9		k1	0.02494	6.83628E-4						
10	400 °C	A	0.9768	0.03773						
11		k1	0.02789	0.00226						
12	500 °C	A	1.00374	0.01613						
13		k1	0.03417	0.00119						
14	600 °C	A	0.9986	0.02496						
15		k1	0.03724	0.00206						
16	700 °C	A	1.01764	0.02621						
17		k1	0.02183	0.00117						
18	800 °C	A	0.98624	0.01375						
19		k1	0.01217	4.11087E-4						
20	900 °C	A	1.00365	0.01474						
21		k1	0.00336	3.01467E-4						
22	1000 °C	A	0.99768	0.00793						
23		k1	0.00172	1.53823E-4						

^{a)} OriginPro 8.5 (OriginLab Corp., Northampton, USA) SW was used for non-linear regression analysis, data from Fig. 4 in the main text.

However, a more detailed inspection showed that the substrate-disappearance curves obtained in the short-time experiments deviate somewhat from the curves predicted from the above model. It was also found from the mass-balance that the sum of all products and reactants in solution (as determined by HPLC) dropped to ca. 80% (in the case of the dephosphorylation on the in-house cerium oxide) or to ca. 90% (dephosphorylation on MKN-025) after an addition of the sorbent to the adenosine phosphate solution. This effect is even more pronounced in the case of the AMP dephosphorylation. It was therefore postulated that some other non-specific process, most probably a non-reactive adsorption, occurs simultaneously with the reactive sorption described above. In this case, a generalized kinetics model involve several equations of the Michaelis-Menten type [1]. An integration of the respective kinetic equations gives equations containing simultaneously the $\ln(y)$ and y terms

$$\ln(Ay + B) + Cy = x + D \quad (12)$$

which can not be solved implicitly [2]. Under certain circumstances (for large x), the solutions based on an approximation of the so-called Lambert W-function may be applied [3, 4]. Eq. (12) may be approximated by a relatively simple equation [5]:

$$y + M = x \left(1 - \frac{\ln x - N}{1 + x} \right) \quad (13)$$

It was found empirically that this equation after a slight modification may be used to fit the experimental data for the disappearance of the adenine phosphates, as is shown in the following figure for AMP.

$$y = \left(1 - \frac{\ln x - N}{1 + x}\right) + Px + M \quad (14)$$

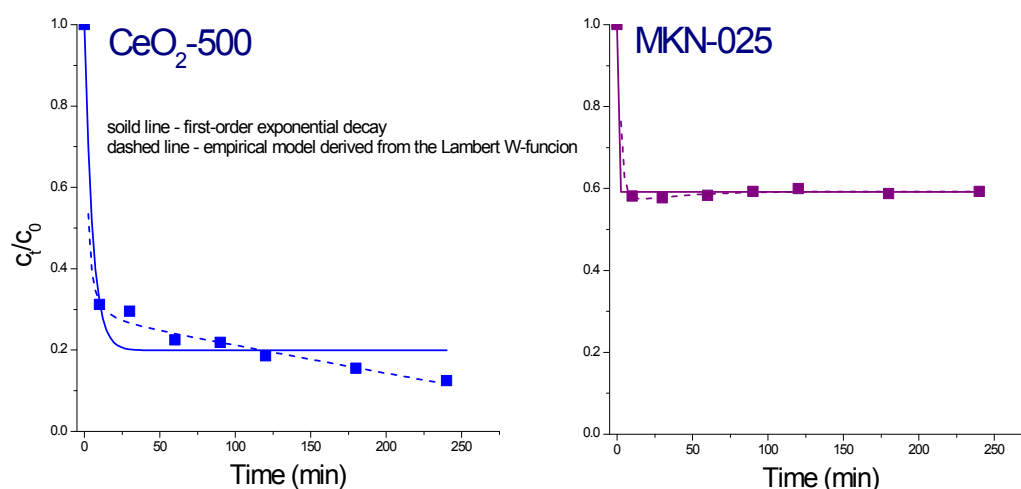


Fig S10. Kinetic dependencies for the dephosphorylation of AMP. Experimental data fitted with the aid of the empirical equation (Eq.(14))

References

- [1] B.J. Johnson, W. Russ Algar, A.P. Malanoski, M.G. Ancona, I.L. Medintz, *Nano Today*, vol. 9, 2014, pp. 102-131.
- [2] M. Goličnik, *Biochemical Engineering Journal*, vol. 53, 2011, pp. 234-238.
- [3] M. Golicnik, *Therapeutic Drug Monitoring*, vol. 33, 2011, pp. 362-365.
- [4] M. Goličnik, F.o.M. Institute of Biochemistry, University of Ljubljana, Ljubljana, Slovenia, F.o.M. Institute of Biochemistry, University of Ljubljana, Vrazov trg 2, 1000 Ljubljana, Slovenia, *Engineering in Life Sciences*, vol. 12, WILEY-VCH Verlag, 2014, pp. 104-108.
- [5] B. Börsch-Supan, *Journal of Research of the National Bureau of Standards - B. Mathematics and Mathematical Physics*, vol. 65B, 1961, pp. 245-250.

6. Interactions of cerium oxide with NAD

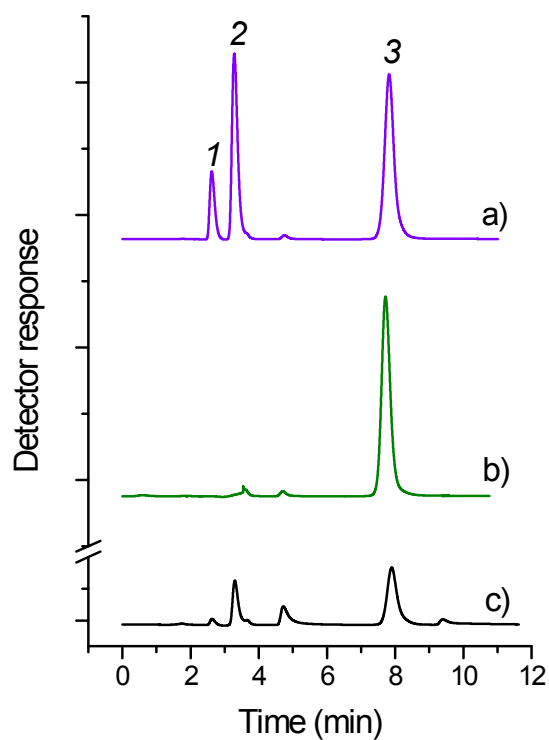


Fig. S11. Decomposition of NAD in the presence of cerium oxide annealed at 500°C. Initial concentrations of NAD 0.002 mol/L,; 0.04 mol/l TRIS buffer with pH = 7.22. Concentrations of cerium oxide 2.0 g/100 mL. a) Model mixture; b) reaction mixture at the beginning of the experiment ($t = 0$); c) Reaction mixture after 6 hours of agitation. Peak identification: 1 - nicotinamide; 2 - adenosine; 3 - NAD. Chromatographic conditions: Column YMC-TRIART DIOL-HILIC, 150×4.6 mm, 5 μ m; mobile phase acetonitrile/ammonium acetate 0.01 mol/L, pH 5.01 (75/25, v/v); detection UV 240 nm.